Title

Heart slice culture system reliably demonstrates clinical drug-related cardiotoxicity.

Authors

Miller, Jessica
Meki, Moustafa
Ou, Qinghui
et al.

Publication Date

2020-11-01

DOI

10.1016/j.taap.2020.115213

Peer reviewed

HHS Public Access

Author manuscript

Toxicol Appl Pharmacol. Author manuscript; available in PMC 2021 November 01.

Published in final edited form as:

Toxicol Appl Pharmacol. 2020 November 01; 406: 115213. doi:10.1016/j.taap.2020.115213.

Heart Slice Culture System Reliably Demonstrates Clinical Drug-Related Cardiotoxicity

Jessica M. Miller[*,1,2], **Moustafa H. Meki**[*,1,2], **Qinghui Ou**[*,1], **Sharon A. George**[*,3], **Anna Gams**[3], **Riham R. E. Abouleisa**[1], **Xian-Liang Tang**[1], **Brooke M. Ahern**[4], **Guruprasad A. Giridharan**[2], **Ayman El-Baz**[2], **Bradford G. Hill**[5], **Jonathan Satin**[4], **Daniel J. Conklin**[5], **Javid Moslehi**[6], **Roberto Bolli**[1], **Alexandre J. S. Ribeiro**[7], **Igor R. Efimov**[3], **Tamer M. A. Mohamed**[1,2,5,8,9,10]

[1]Institute of Molecular Cardiology, Department of Medicine, University of Louisville, KY, USA

[2]Department of Bioengineering, University of Louisville, KY, USA

[3]Department of Biomedical Engineering, The George Washington University, Washington, DC, USA

[4]Department of Physiology, University of Kentucky, KY, USA

[5]Envirome Institute, Diabetes and Obesity Center, Department of Medicine, University of Louisville, KY, USA

[6]Division of Cardiology, Cardio-Oncology Program, Vanderbilt University Medical Center, 2220 Pierce Avenue, Nashville, USA.

[7]U.S. Food and Drug Administration, Center for Drug Evaluation and Research, Office of Translational Science, Office of Clinical Pharmacology, Division of Applied Regulatory Science, Silver Spring, MD, USA

[8]Department of Pharmacology and Toxicology, University of Louisville, KY, USA

[9]Institute of Cardiovascular Sciences, University of Manchester, UK

[10]Faculty of Pharmacy, Zagazig University, Egypt

Abstract

Correspondence to: Tamer M A Mohamed, Institute of Molecular Cardiology, University of Louisville, 580 South Preston Street, Louisville, KY 40202. tamer.mohamed@louisville.edu; Igor R Efimov, Department of Biomedical Engineering, The George Washington University, 5000 Science and Engineering Hall, Washington, DC 20052, USA. efimov@gwu.edu; Alexandre J. S. Ribeiro, U.S. Food and Drug Administration, Center for Drug Evaluation and Research, Office of Translational Science, Office of Clinical Pharmacology, Division of Applied Regulatory Science, Silver Spring, MD, USA. Alexandre.Ribeiro@fda.hhs.gov.

*Authors equally contributed to the work.

Author contributions

J.M.M, M.H.M, Q.O, S.A.G.: collection and analysis of data, manuscript writing, and final approval of manuscript; A.G., R.R.E.A., X-L.T., B.M.A. collection and analysis of data; G.A.G., A.E., B.G.H., J.S., D.J.C., J.M., R.B., A.J.S.R, I.R.E, and T.M.A.M: conception and design, manuscript writing, and final approval of manuscript.

Competing Interests

TMAM, holds equities in Tenaya Therapeutics. GAG, is consultant for NuPulseCV. The other authors report no conflicts.

Disclaimer

This article reflects the views of the authors and should not be construed to represent the views or policies of the FDA

The limited availability of human heart tissue and its complex cell composition are major limiting factors for the reliable testing of drug efficacy and toxicity. Recently, we developed functional human and pig heart slice biomimetic culture systems that preserve the viability and functionality of 300 μm heart slices for up to 6 days. Here, we tested the reliability of this culture system for testing the cardiotoxicity of anti-cancer drugs. We tested three anti-cancer drugs (doxorubicin, trastuzumab, and sunitinib) with known different mechanisms of cardiotoxicity at three concentrations and assessed the effect of these drugs on heart slice viability, structure, function and gene expression. Slices incubated with any of these drugs for 48 h showed diminished in viability as well as loss of cardiomyocyte structure and function. Mechanistically, RNA sequencing of doxorubicin-treated tissues demonstrated a significant downregulation of cardiac genes and upregulation of oxidative stress responses. Trastuzumab treatment downregulated cardiac muscle contraction-related genes consistent with its clinically known effect on cardiomyocytes. Interestingly, sunitinib treatment resulted in significant downregulation of angiogenesis-related genes, in line with its mechanism of action. Similar to hiPS-derived-cardiomyocytes, heart slices recapitulated the expected toxicity of doxorubicin and trastuzumab; however, slices were superior in detecting sunitinib cardiotoxicity and mechanism in the clinically relevant concentration range of 0.1-1 μM. These results indicate that heart slice culture models have the potential to become a reliable platform for testing and elucidating mechanisms of drug cardiotoxicity.

Introduction

Toxicity related to interruptions in cardiomyocyte electrical activity and contractility is a major cause of drug withdrawals from the market[1-3]. In the last decade, there has been an explosion of cancer therapies, several of which often lead to cardiotoxicity causing cardiomyopathy, arrhythmias, irreversible heart failure, or death[4]. For example, both traditional (e.g., anthracyclines and radiation) and targeted (e.g., trastuzumab) breast cancer therapies can result in cardiovascular complications in a subset of patients[5, 6]. The cardiovascular effects of newer classes of drugs, such as CDK4/6 inhibitors and PI3K inhibitors, remain unclear[7, 8]. The recent higher cancer survival is partially offset by increased morbidity and mortality related to the cardiotoxic side effects of anti-cancer therapeutics[9]. Hence, a close collaboration between cardiologists and oncologists (in the emerging field of cardio-oncology) aims to make these complications manageable to ensure that patients can be treated as safely and effectively as possible, according to the International Council for Harmonization of Technical Requirements for Pharmaceuticals for Human Use (ICH) guidelines[10]. Therefore, there is a growing need for better testing platforms, both for assessing cardiovascular toxicity and for elucidating mechanisms by which cancer therapies promote cardiotoxicity[11, 12].

Detection of cardiotoxic effects of drug candidates requires the use of *in vivo* and *in vitro* studies prior to clinical trials[13]. Therefore, there is an urgent need for reliable preclinical screening strategies for cardiovascular toxicity associated with emerging cancer therapies prior to human clinical trials. Animal models can fail to predict adverse cardiac effects of drugs[14, 15], can be expensive, and may not replicate many of the biochemical properties and hemodynamic aspects of the human heart and circulation[16-18]. Recently, human induced

pluripotent stem cell derived cardiomyocytes (hiPSC-CMs) have been used to assess drug-induced cardiotoxicity[19, 20]. However, these cells have several fetal-like properties that can impact the reliability of predicting clinical drug side effects on adult human heart. The development of hiPSC-CMs microtissues is a promising effort to generate more mature phenotypes, but it is still a work in progress[19, 20]. Although microtissues express some gap junction proteins and exhibit a degree of cell-to-cell coupling, they do not fully recapitulate the syncytium observed in the intact heart[21]. A less common approach has been the use of isolated primary human cardiomyocytes. While these cells are functionally mature, and can be used for high-throughput testing, they readily dedifferentiate in culture, thereby limiting their use for cardiotoxicity studies[22]. The adult human heart tissue is structurally more complicated, being composed of a heterogeneous mixture of cell types including cardiomyocytes, endothelial cells, smooth muscle cells, and various types of stromal fibroblasts linked together with a sophisticated three-dimensional network of extracellular matrix proteins[23]. This heterogeneity of the non-cardiomyocyte cell population[24-26] in the adult heart is a major obstacle in modeling heart tissue using individual cell types. Human ventricular wedge preparations have also been used to study electrophysiology[27, 28]. However, the wedge preparations are typically large in size and have functional viability of only several hours, limiting their high-throughput applicability.

These major limitations highlight the importance of developing optimal methods to enable the culture of intact cardiac tissue for studies involving physiological and pathological conditions[21]. Culturing human heart slices has shown promise in extending the functionality and viability of cardiac tissue. By retaining the normal tissue architecture, the multi-cell type environment, and the 3-dimensional structure, tissue slices can more faithfully replicate the organ-level adult cardiac physiology in terms of normal conduction velocity, action potential duration, and intracellular calcium dynamics[29, 30]. Recently, we developed (through optimization of the medium and culture conditions with continuous electrical stimulation at 1.2 Hz and oxygenation of the culture medium) a novel biomimetic culture system that maintains full viability and functionality of both human and pig heart slices (300 μm thickness) for 6 days in culture[31]. In the present study, we tested the reliability of this culture system in recapitulating clinical toxicity and potentially delineating the mechanisms of known cardiotoxic drugs. To this end, we selected three anticancer drugs with known adverse cardiac side effects: doxorubicin, an anthracycline with a long history of cardiotoxicity; trastuzumab, a monoclonal antibody target HER2; and, sunitinib, a small molecule multi-targeted tyrosine kinase inhibitor (TKI) with potent activity against VEGF and PDGF receptors[6]. All three drugs have been associated with cardiomyopathy through different mechanisms[6]. These three drugs were selected because doxorubicin and trastuzumab are shown to be cardiotoxic in hiPSC-CMs[32, 33]; however, nanomolar concentrations of sunitinib do not cause any cardiotoxicity phenotype in hiPSC-CMs[34]. Therefore, we first confirmed previously reported cardiotoxic phenotype of doxorubicin and the absence of sunitinib effect, at low concentrations, in hiPS-CMs[34]. In pig heart slices, we tested three different concentrations of each drug in ten-fold incremental values, with the lowest dose being the most clinically relevant, and assessed the effect of these drugs on heart slice viability, structure, function and gene expression. As the maximum blood concentration of doxorubicin ranges between 100nM-300nM[35], we used 100nM, 1μM, 10μM

concentrations. We used 1μg/mL, 10μg/mL and 100μg/mL concentrations for trastuzumab as the blood level is ranging between 1-10μg/mL[36]. Sunitinib concentrations of 100nM, 1μM, and 10μM were used as the normal blood concentration range is 100nM-200nM[37]. Finally, we assessed the ability and reproducibility of human heart slices in demonstrating the cardiotoxic effect and mechanism of doxorubicin between different human subjects.

Methods

Apoptotic assay on hiPSC-CMs

hiPSC-CMs (iCell Cardiomyocytes[2]) were purchased from Cellular Dynamics (currently FujiFilm Inc.). These hiPSC-CMs have been selected after differentiation using an a-MHC-Blastocidin selection cassette. This strategy yields nearly 100% pure hiPSC-CMs. Following vendor recommendations, hiPSC-CMs were seeded on fibronectin-coated plates and cultured in maintenance medium. hiPSC-CMs were exposed to a range of concentrations of doxorubicin (cardiotoxin), sunitinib (cardiotoxic TKI), aspirin (non-toxic drug), erlotinib (non-cardiotoxic TKI) over 48 h. DMSO in the medium at a concentration of 0.1% (v/v) was used as a control condition for each drug. Live cell brightfield and fluorescent images for time-lapse experiments were acquired using the Incucyte® S3 Live Cell Analysis System (Essen Bioscience / Sartorius) running version 2019A (20191.1.6976.19779). Plates were imaged hourly following initiation of drug treatment. Three images at set locations within each well were acquired at 10x magnification for each time point. For fluorescent imaging of apoptosis, the Incucyte Caspase-3/7 Green dye (Essen Bioscience 4440) was added to the media/drug cocktail at a concentration of 5 μM for the duration of the assay. Analysis of apoptosis using the Caspase 3/7 fluorescent dye was performed using the Incucyte software. Parameters were set to quantify green fluorescent intensity metrics and areas of high signal intensity indicated cell death.

Harvesting porcine heart tissue

All animal procedures were in accordance with the institutional guidelines and approved by the University of Louisville Institutional Animal Care and Use Committee. The protocol for harvesting pig hearts has been described in detail[31, 38]. Briefly, pigs were deeply anesthetized the with 5% isoflurane, and the heart was quickly excised and clamped at the aortic arch and perfused with 1L sterile cardioplegia solution (110 mM NaCl, 1.2 mM $CaCl_2$, 16 mM KCl, 16 mM $MgCl_2$, 10 mM $NaHCO_3$, 5 units/mL heparin, pH to 7.4). The heart was preserved on an ice-cold cardioplegic solution and immediately transported to the lab on wet ice.

Human heart slices

Donor hearts that were not used in cardiac transplantation were acquired through our collaboration with the Washington Regional Transplant Community. Human cardiac organotypic slices were prepared as previously described[39].

Heart slicing and culturing

Slicing and culturing of 300 μm thick heart tissue slices were performed as previously described[31, 38]. A refined oxygenated growth medium was used (Medium 199, 1x ITS

supplement, 10% FBS, 5 ng/mL VEGF, 10 ng/mL FGF-basic, and 2x Antibiotic-Antimycotic), and changed 3 times/day. Sunitinib (Tocris Inc.) (100 nM, 1μM, and 10 μM), trastuzumab (InvivoGen Inc.) (1 μg, 10 μg, and 100 μg), or doxorubicin (Sigma Millipore Inc.) (100 nM, 1μM, and 10 μM, and 50 μM) was added freshly to the culture medium at each medium change. Control slices received DMSO at the same dilution factor as the matched drug-treated slices. For detailed protocols regarding slicing and culturing heart slices, please see the Supplementary Methods.

MTT viability assay

For the MTT assay, we used the Vybrant ® MTT Cell Proliferation Assay kit (Thermo Scientific) following the manufacturer's protocol with slight modifications. Using a sterile scalpel, each heart slice was cut into 2 ~0.5 cm^2-sized sections for the MTT assay. The heart slice segments were placed into a single well of a 12-well plate containing 0.9 mL growth media with 0.1 mL of reconstituted MTT substrate that was prepared according to the manufacturer's protocol. The tissue was incubated at 37°C for 3 h. During this time, viable tissue metabolized the MTT substrate and produced a purple insoluble formazan compound. To extract formazan from the tissue slices, the tissue was transferred into 1 mL of DMSO and incubated at 37°C for 15 min. The resulting solution was purple in color. This solution was then transferred into a clear bottom 96-well plate in triplicate at 3 dilutions: 1:2, 1:5, and 1:10. The intensity of the purple color was measured using Cytation 1 plate reader (BioTek) at 570 nm. The readings were normalized to the weight of each heart tissue section and converted into OD/mg tissue. The 3 dilutions of the solution were performed to correct for any possible signal saturation and the average of all readings was normalized to their dilution factor.

Heart slice fixation, mounting and immunofluorescence

Heart slices were fixed with 4% paraformaldehyde for 48 h. Fixed tissue was dehydrated in 10% sucrose for 1 h, 20% sucrose for 1 h, and 30% sucrose for overnight. The dehydrated tissue was then embedded in optimal cutting temperature compound (OCT compound) and gradually frozen in isopentane/dry ice bath. OCT embedded blocks were stored at −80°C until sectioning. Sections (8 μm) were cut and immunolabeled for target proteins. To remove the OCT compound, the slides were heated for 5 min at 95°C until the OCT compound melted. Then 1 mL of PBS was added to each slide and incubated at RT for 10-30 min until the OCT compound washed off. Sections were then permeabilized by incubating for 30 min in 0.1% Triton-X in PBS at RT. The Triton-X was removed, and non-specific antibody binding of the sections were blocked with 3% BSA solution for 1 h at RT. After washing off the BSA with PBS, each section was marked off with a wax pen. After marking sections, the primary antibodies (1:200 dilution in 1% BSA) connexin 43 (Abcam; #AB11370), and troponin-T (Thermo Scientific; #MA5-12960)] were added to each section and incubated for 90 min at RT. The primary antibodies were washed off with PBS three times followed by the addition of the secondary antibodies (1:200 dilution in 1% BSA) anti-Ms AlexaFluor 488 (Thermo Scientific; #A16079), anti-Rb AlexaFluor 594 (Thermo Scientific; #T6391) and incubated for 90 min at RT. The secondary antibody was removed by washing the sections 3 times with PBS. To distinguish the *bona fide* target staining from the background, we used a secondary antibody only as a control. After 3 PBS washes, DAPI was added for 15 min. The

sections were washed again 3 times with PBS. Finally, slices were mounted in vectashield (Vector Laboratories) and sealed with nail polish. All immunofluorescence imaging and quantification were performed using a Cytation 1 high content imager and the fluorescent signal quantification and masking were performed using the Gen5 software.

Calcium-transient assessment

Calcium transients were assessed as previously described[31]. Briefly, heart slices were loaded with Fluo-4 for 30 min at room temperature before being transferred to the imaging chamber. The loading solution contained a 1:10 mixture of 5 mM Fluo-4 AM in dry DMSO and PowerloadTM concentrate (Invitrogen), which was diluted 100-fold into extracellular Tyrode's solution (NaCl 140mM; KCl 4.5mM; glucose 10mM; HEPES 10mM; $MgCl_2$ 1mM; $CaCl_2$ 1.8mM; 2x Antibiotic-Antimycotic; pH 7.4). An additional 20 min were allowed for de-esterification before recordings were made. Contractions and calcium transients were evoked by applying voltage pulses at 1 Hz between platinum wires placed on either side of the heart slice and connected to a field stimulator (IonOptix, Myopacer). Fluo-4 fluorescence transients were recorded via a standard filter set (#49011 ET, Chroma Technology). Resting fluorescence was recorded after cessation of pacing, and background light was obtained after removing the heart slice from the field of view at the end of the experiment. All analyses of calcium transients were based on calcium transients recorded from single cardiomyocytes within the heart slice and the calcium transient's amplitude was assessed as the average of 10 consecutive beats from each cell. Calcium transients and amplitude was assessed following normalization to the basal florescence of each cell and represented as F/F_0.

Contractile function monitoring of heart slices using CardioExcyte 96 system

Circular punches (6mm diam.) from the heart slices were generated using Integra™ Miltex™ Standard Biopsy Punches (Fisher Inc.), and a single punch was placed in a well of the NSP-96, CardioExcyte 96 Sensor Plates with extra stimulation electrode. The NSP-96 plate was maintained in the CardioExcyte 96 system at 37˚C and 5% CO_2. The heart slices were electrically stimulated at 1Hz during the course of the recording. Impedance recordings were performed every 2 min for 1 h. The data were analyzed with CardioExcyte 96 analysis software.

RNA Sequencing

RNA was isolated from the heart slices by using the Qiagen miRNeasy Micro Kit, #210874, following the manufacturer's protocol after homogenization of tissue in Trizol. RNAseq library preparation, sequencing, and data analysis were performed as described previously[31].

Optical Mapping

For single parameter voltage optical mapping, slices were incubated with Di-4-ANEPPS (30 μl of stock solution at 1.25 mg/mL diluted to 1 mL with recovery solution [140 mM NaCl, 4.5 mM KCl, 1 mM MgCl2, 1.8 mM CaCl2, 10 mM glucose, 10 mM HEPES, 10 mM BDM; pH 7.4]). Slices were paced at 1 Hz frequency, 2 ms duration at an amplitude of 1.5x the threshold for stimulation using a platinum bipolar pacing wire positioned at the center of

the slice. Slices were excited using excitation light at 520 ± 5 nm and the emitted light was collected by a tandem lens optical mapping system, filtered using a 610 ± 20 nm filter and recorded using the SciMedia Ultima L-type CMOS cameras.

Optical signals were analyzed as previously described[39, 40]. Briefly, activation times were defined as the time of maximum first derivative of the fluorescence signal during the upstroke. End of action potential and calcium transients were defined as the point where the signal returns to 80% of its total signal amplitude. Conduction velocity was determined in the transverse direction of propagation using activation times and known interpixel resolution.

Cap analysis of gene expression

For high-throughput analysis of transcriptional starting point and identification of promoter usage, we performed cap analysis of gene expression (CAGE). Total RNA from the cultured slices was extracted using the RNeasy Fibrous Tissue Mini Kit according to the manufacture's protocol. Library preparation and sequencing with HiSeq2500 was performed according to the Morioka *et al* protocol[41]. Read mapping was performed with Burrows-Wheeler Aligner[42]; subsequent analysis of reads into decomposition peak identification (DPI) and transcription start site-like peaks was performed with *DPI1* (https://github.com/hkawaji/dpi1/) followed by *TomeTools TSSClassifier* (https://sourceforge.net/projects/tometools/). Differential expression analysis was performed with *edgeR*[43], gene ontology (GO) with *limma*[44], and heatmap plotting with *pheatmap* (https://CRAN.R-project.org/package=pheatmap).

Results

hiPSC-CMs demonstrate cardiotoxic effects of doxorubicin but not sunitinib at the clinically relevant nanomolar concentrations

In clinical settings, cancer therapies can lead to cardiomyopathy due to direct cardiomyocyte death as well as effects on non-cardiomyocytes in the heart[34, 45-47]. A major distinction between the heart slice preparation and hiPSC-CMs is the retention of multiple cell types in heart slices. It has been reported hiPSC-CMs demonstrate the cardiotoxic phenotype of doxorubicin in nanomolar concentrations but not sunitinib at nanomolar concentrations[34]. First, we reproduced these findings, wherein we tested for effects of different concentrations of doxorubicin, and sunitinib on hiPS-CMs viability using caspapse3/7 apoptosis assay over 48 h. Aspirin and erlotinib (non-cardiotoxic TKI) were used as negative controls (Figure 1). Consistent with the previous report[34], sunitinib did not show any cardiotoxicity in hiPSC-CMs at 500 nM or 1 μM concentrations as assessed by caspase3/7 apoptosis assay (Figure 1d-f). However, sunitinib at 60 μM showed an acute apoptotic response within 1 h of addition, resulting in no more fluorescence detected over the course of the experiment at this concentration (Figure 1d-f). However, doxorubicin, even at low concentrations (e.g., 500 nM), induced the expected cardiotoxicity in hiPSC-CMs, while the negative controls [aspirin and erlotinib (non-cardiotoxic TKI)] had no effect on hiPSC-CMs up to 60 μM (Figure 1a-c).

Effect of cardiotoxins on heart slices viability and cardiomyocyte integrity

To assess heart slice viability, we used the MTT assay to quantify the activity of the mitochondrial NAD(P)H-dependent cellular oxidoreductase enzymes, as a measure of metabolic activity of the heart slice[31]. Thus, it is expected that apoptotic and non-apoptotic mechanisms of cytotoxicity will be captured by this more general measure of cell viability. Pig heart slice exposure to these concentrations of cardiotoxins for 48 h resulted in a significant decline in the general viability of the tissue (Figure 2a). Structurally, following the tissue exposure to doxorubicin at the lowest concentration, there was a decrease in the expression of the gap junction protein, connexin-43, and the sarcomeric protein, troponin T, expression (Figure 2b). Heart slices treated with trastuzumab at the lowest concentration showed disruption in connexin-43 localization at the gap junction accompanied by a lower level of troponin T expression (Figure 2b). Interestingly, low concentration sunitinib treatment did not appear to affect the structure of slices; however, higher concentrations disrupted connexin-43 localization and diminished troponin T expression (Figure 2b).

Effect of cardiotoxins on heart slices calcium homeostasis and contractile function

We next tested the effects of cardiotoxins on calcium homeostasis within pig heart slices after 48 h exposure. The highest tested concentrations of cardiotoxins completely abolished calcium transients (Supp Movie 3, 4, 6, 7, 9 and 10) compared with the control (Supp movie 1). However, as the lower concentrations are more clinically relevant, these exposures demonstrated several of the clinically observed effects on cardiac contractility and rhythm[6]. Treatment with 100 nM doxorubicin abolished calcium transients indicating direct cardiomyocyte damage (Figure 3a-b, Supp movie 2). Trastuzumab (1 μg) (Figure 3a-b, Supp movie 5) or sunitinib (100 nM) (Figure 3a-b, Supp movie 8) treatment severely disrupted calcium homeostasis within the heart slices. In line with the disruption in calcium homeostasis, contractile function (measured by impedance) was completely suppressed in all heart slices treated at the lowest concentration of the cardiotoxins for 48 h (Figure 3c).

Mechanistic understanding of the cardiotoxic effects

Transcriptomic analyses were performed to probe the mechanisms underlying the responses of the pig heart slice to cardiotoxins. The most significant up/downregulated gene ontology (GO) terms for slices treated with 100 nM of doxorubicin are shown in Figure 4a-c. The top downregulated GO terms were genes responsible for cardiac muscle and development as well as cell division genes. The top upregulated GO terms were genes involved in oxidation/reduction and inflammatory responses, which is consistent with the known induction of free radicals by doxorubicin. Figure 5a-c shows the up/downregulated genes in heart slices treated with 1 μg trastuzumab for 48 h. The downregulated genes are mainly contractile genes indicative of a direct effect on cardiomyocyte structure. Figure 6a-c shows the up/downregulated GO terms in heart slices treated with 100 nM sunitinib. Sunitinib treatment significantly downregulated angiogenesis-related genes, which is consistent with reported changes in VEGF/PDGF signaling[46, 48].

Human heart slices can reliably and consistently predict doxorubicin cardiotoxicity

Although the results of the experiments described above indicate that pig heart slices can be used to test the effects of drugs on cardiac viability, structure, calcium dynamics, and gene expression, ultimate goal in the field is to predict cardiotoxicity in the human heart. Thus, we next used healthy human heart tissue to examine doxorubicin cardiotoxicity. To ensure consistency between human hearts in demonstrating the mechanism of doxorubicin cardiotoxicity, we used 3 female and 8 male hearts with an age range between 28-70 years old and with various causes of death (Figure 7a). Consistent with the pig heart data, doxorubicin promoted electrophysiological remodeling in human heart slices. Exposure of the slices to 50 μM doxorubicin for 24 h led to significant slowing of cardiac conduction velocity in the transverse direction of propagation[40] (Figure 7b-c). These results are consistent with reports of acute electrophysiologic alterations in some patients treated with doxorubicin[49]. Furthermore, Cap analysis of gene expression (CAGE) transcriptome analysis revealed 1433 differentially expressed genes in control and 2172 differentially expressed genes at the promoter level in doxorubicin-treated human cardiac slices as illustrated (Figure 7d). GO analysis revealed that most differentially expressed genes were associated with DNA repair, oxidation-reduction, mitochondria viability and oxidative phosphorylation; changes likely related to the damage of the energetic capacity of the cardiomyocytes (Figure 7e). Hierarchical clustering analysis illustrated different clustering of control and doxorubicin-treated human cardiac organotypic slices (Figure 7f). Importantly, these analyses showed the consistency of the transcriptomic response to doxorubicin across different human subjects (Figure 7f).

Discussion

Drug-induced cardiotoxicity is a major cause of drug attrition[3]. This problem is particularly relevant to new cancer therapies, resulting in the burgeoning field of cardio-oncology[50]. Therefore, there is a pressing need for predictable preclinical screening strategies for cardiovascular toxicities associated with emerging drugs prior to clinical trials[11, 12]. The recent consideration of hiPSC-CMs for testing drug toxicity provides a partial solution in some contexts but does not solve the overall need for predicting the diversity of functional cardiac toxicity, e.g., effects on endothelial cells, microvasculature or smooth muscle cells[19, 20]. In addition to fetal-like properties, a single cell type does not replicate the complexity of a 3-D heart organ that contains multiple cell types and biological connections. In the current study, we demonstrate diverse clinical cardiotoxic phenotypes and mechanisms using three mechanistically different cancer therapies with cardiotoxic potential in a 3-D heart slice culture model.

The first drug that we tested was an anthracycline, which is a class of antibiotics discovered over 60 years ago and used to treat many different cancers[51]. Doxorubicin is one of the commonly used anthracyclines for the treatment of lymphoma, leukemia, sarcoma, and breast cancer[51, 52]. The anticancer activity of doxorubicin results from DNA and RNA synthesis disruption[51], attenuated DNA repair[53], and generation of free radicals which damage DNA[54]. Even though doxorubicin is an effective and commonly used anticancer therapy, its use is limited by its cardiotoxicity. Between 5% and 23% of the patients that

receive doxorubicin develop diminished exercise capacity and progressive heart failure symptoms[55, 56]. Toxicity mechanisms of doxorubicin are still poorly understood, despite being a compound studied extensively for decades; however, doxorubicin has been found to induce multiple forms of direct cardiomyocyte injury as a result of free radical production induced by the quinone group[57]. This direct damage to cardiomyocytes has been demonstrated in hiPSC-CMs[32, 34]. Consistent with these reports, our pig and human heart slice models recapitulated the known response to doxorubicin. Phenotypically, doxorubicin induces direct cardiomyocyte damage as shown by a decline in MTT viability assay, decreases connexin 43 and troponin T expression, abolished calcium transients, and reduced contractility. Mechanistically, RNAseq and CAGE transcriptomics analyses show downregulation of genes responsible for cardiac development, mitochondria viability and oxidative phosphorylation and cellular division, with upregulation of genes involved in oxidation/reduction and inflammatory responses, which are congruent with the oxidative stress known to be induced by doxorubicin[34].

The second cardiotoxin is a HER2-targeted agent (Trastuzumab), a humanized monoclonal antibody targeting HER2/*neu* receptors (also known as ERBB2) and the first approved HER2-targeted agent[58]. Trastuzumab exerts its anticancer effect through blocking the activation of the HER2(ERBB2)/*neu* receptor, leading to the inhibition of epidermal growth factors/HER2 ligand receptor activity and disrupting the phosphorylation of tyrosine kinases which are critical regulators of the cell cycle[58]. It has been noted that trastuzumab treatment results in asymptomatic cardiac dysfunction and, less often, symptomatic heart failure in some patients[59]. Trastuzumab-induced cardiotoxicity is thought to be driven by disruption of ERBB2/neuregulin signaling in cardiomyocytes, which is critical for normal myocyte growth, survival, and homeostasis[60]. The trastuzumab-induced direct cardiomyocyte damage phenotype and mechanism is modeled recently in hiPSC-CMs[33, 61]. Consistent with these reports, pig heart slices treated with trastuzumab show direct cardiomyocyte damage, as evidenced by decline in connexin 43 and troponin T expression and disruption of calcium homeostasis and contractile function. Mechanistically, RNAseq confirmed the direct damage in cardiomyocytes and downregulation of cardiac contractile gene expression.

Sunitinib was the third cardiotoxin tested; it is a TKI, which inhibits angiogenesis through inhibition of vascular endothelial growth factor (VEGF). Sunitinib is associated with hypertension, vascular disease, as well as cardiomyopathy[62]. Cardiac systolic dysfunction, which has been observed in 10-15% of patients treated with sunitinib and sorafenib,[48] has been attributed to the disruption of the coronary microvascular pericytes leading to cardiomyocyte hypoxia[46] and cardiomyopathy[63]. It was not possible to model these indirect effects using hiPSC-CMs, as nanomolar concentrations of sunitinib treatment had no obvious cardiotoxic effects on hiPSC-CMs. This is likely due to its indirect effect on cardiomyocytes as indicated by our data (Figure 1) and others[34]. Although in our heart slice system sunitinib (as low as 100nM) caused no major phenotypic damage to cardiomyocyte structure, as indicated by connexin 43 and troponin T expression, it significantly disrupted contractile function and calcium homeostasis. Mechanistically, RNAseq data from heart slices treated with 100nM sunitinib demonstrate clear disruption of the angiogenic gene program, which is consistent with its known clinical effects[46, 48].

In conclusion, the results of this study suggest that the heart slice culture system is a promising platform for modeling cardiotoxicity phenotypes and mechanisms. These data suggest that this system will be useful to test acute and subacute cardiotoxicity of new therapeutics.

Limitations of the study

We consider this work a proof of concept study that demonstrates the ability of heart slices to reflect clinical phenotypes of cardiotoxins. We used only three cardiotoxins at three different concentrations and assessed effects at one time point (48 h). At this time point, however, there is significant functional cardiotoxicity even at the lowest concentration tested as shown by reduction of calcium transients and contractile function. Further studies could address a more in-depth time course as well as testing other cardiotoxins. Furthermore, studies to test cardiotoxicity in enhanced cardiac function models are needed. Another limitation of the study is that we can only record conduction velocity by optical mapping as described in Figure 7b-c. Taking in consideration that electrophysiology is of high relevance for predicting drug arrhythmogenic potential, action potential recordings from the whole tissue would be informative. Indeed, a recent study established a glass microelectrode technique to perform patch clamping on the whole heart[64]. Neverthless, further studies are required to adapt this microelectrode technology for recording action potentials in heart slices. Another limitation is that heart slice technology is technically and financially demanding, which may limit its general or widespread use. To this end, the authors have recently published detailed video protocols to promote the use of this technology[38, 40]. A major limitation of the heart slice technology is the relatively short viability in culture (6 days), which makes it suitable for only acute and subacute cardiotoxicity testing but not for chronic toxicity testing. Further efforts to prolong the viability in culture are needed.

Supplementary Material

Refer to Web version on PubMed Central for supplementary material.

Acknowledgments

TMAM is supported by NIH grants R01HL147921 and P30GM127607 and American Heart Association grant 16SDG29950012. The authors also acknowledge NIH grants P30GM127607 (BGH), R01HL130174 (BGH), R01HL147844 (BGH), R01ES028268 (BGH), GM127607 (DJC), P01HL78825 (RB, BGH) and UM1HL113530 (RB), Leducq Foundation RHYTHM grant (IRE), R01HL126802 (IRE), R44HL139248 (IRE) and an American Heart Association Postdoctoral fellowship (19POST34370122) to SAG. We also acknowledge the USA Department of Defense for the grant W81XWH-20-1-0419 (JS, TMAM). We acknowledge the guidance of Ruslan Deviatiiarov from the Institute of Fundamental Medicine and Biology. Kazan Federal University, Russia in the Cap Analysis of Gene expression data analysis.

References

1. Mladenka P, Applova L, Patocka J, Costa VM, Remiao F, Pourova J, Mladenka A, Karlickova J, Jahodar L, Voprsalova M, Varner KJ, Sterba M, Tox OER, Researchers CHK and Collaborators. Comprehensive review of cardiovascular toxicity of drugs and related agents. Med Res Rev. 2018;38:1332–1403. [PubMed: 29315692]
2. Kocadal K, Saygi S, Alkas FB and Sardas S. Drug-associated cardiovascular risks: A retrospective evaluation of withdrawn drugs. North Clin Istanb. 2019;6:196–202. [PubMed: 31297490]

3. Onakpoya IJ, Heneghan CJ and Aronson JK. Post-marketing withdrawal of 462 medicinal products because of adverse drug reactions: a systematic review of the world literature. BioMed Central Medicine. 2016;14:10.
4. Mercuro G, Cadeddu C, Piras A, Dessi M, Madeddu C, Deidda M, Serpe R, Massa E and Mantovani G. Early epirubicin-induced myocardial dysfunction revealed by serial tissue Doppler echocardiography: correlation with inflammatory and oxidative stress markers. The oncologist. 2007;12:1124–33. [PubMed: 17914082]
5. Lenneman CG and Sawyer DB. Cardio-Oncology: An Update on Cardiotoxicity of Cancer-Related Treatment. Circulation Research. 2016;118:1008–20. [PubMed: 26987914]
6. Moslehi JJ. Cardiovascular Toxic Effects of Targeted Cancer Therapies. The New England journal of medicine. 2016;375:1457–1467. [PubMed: 27732808]
7. Yang B and Papoian T. Preclinical approaches to assess potential kinase inhibitor-induced cardiac toxicity: Past, present and future. J Appl Toxicol. 2018;38:790–800. [PubMed: 29369373]
8. Knudsen ES and Witkiewicz AK. The Strange Case of CDK4/6 Inhibitors: Mechanisms, Resistance, and Combination Strategies. Trends Cancer. 2017;3:39–55. [PubMed: 28303264]
9. Han X, Zhou Y and Liu W. Precision cardio-oncology: understanding the cardiotoxicity of cancer therapy. NPJ precision oncology. 2017;1:31. [PubMed: 29872712]
10. Ponce R ICH S9: Developing anticancer drugs, one year later. Toxicol Pathol. 2011;39:913–5. [PubMed: 21859887]
11. Sheng CC, Amiri-Kordestani L, Palmby T, Force T, Hong CC, Wu JC, Croce K, Kim G and Moslehi J. 21st Century Cardio-Oncology: Identifying Cardiac Safety Signals in the Era of Personalized Medicine. Journal of the American College of Cardiology: Basic to Translational Science. 2016;1:386–398. [PubMed: 28713868]
12. Bellinger AM, Arteaga CL, Force T, Humphreys BD, Demetri GD, Druker BJ and Moslehi JJ. Cardio-Oncology: How New Targeted Cancer Therapies and Precision Medicine Can Inform Cardiovascular Discovery. Circulation. 2015;132:2248–58. [PubMed: 26644247]
13. Hughes JP, Rees S, Kalindjian SB and Philpott KL. Principles of early drug discovery. British journal of pharmacology. 2011;162:1239–49. [PubMed: 21091654]
14. Van Norman GA. Limitations of Animal Studies for Predicting Toxicity in Clinical Trials: Is it Time to Rethink Our Current Approach? Journal of the American College of Cardiology: Basic to Translational Science. 2019;4:845–854. [PubMed: 31998852]
15. Van Norman GA. Limitations of Animal Studies for Predicting Toxicity in Clinical Trials: Part 2: Potential Alternatives to the Use of Animals in Preclinical Trials. Journal of the American College of Cardiology: Basic to Translational Science. 2020;5:387–397. [PubMed: 32363250]
16. Hearse DJ and Sutherland FJ. Experimental models for the study of cardiovascular function and disease. Pharmacological research. 2000;41:597–603. [PubMed: 10816328]
17. Houser SR, Margulies KB, Murphy AM, Spinale FG, Francis GS, Prabhu SD, Rockman HA, Kass DA, Molkentin JD, Sussman MA and Koch WJ. Animal Models of Heart Failure. Circulation Research. 2012;111:131–150. [PubMed: 22595296]
18. Clark M and Steger-Hartmann T. A big data approach to the concordance of the toxicity of pharmaceuticals in animals and humans. Regul Toxicol Pharmacol. 2018;96:94–105. [PubMed: 29730448]
19. Gintant G, Burridge P, Gepstein L, Harding S, Herron T, Hong C, Jalife J and Wu JC. Use of Human Induced Pluripotent Stem Cell-Derived Cardiomyocytes in Preclinical Cancer Drug Cardiotoxicity Testing: A Scientific Statement From the American Heart Association. Circulation Research. 2019;125:e75–e92. [PubMed: 31533542]
20. Pang L, Sager P, Yang X, Shi H, Sannajust F, Brock M, Wu JC, Abi-Gerges N, Lyn-Cook B, Berridge BR and Stockbridge N. Workshop Report: FDA Workshop on Improving Cardiotoxicity Assessment With Human-Relevant Platforms. Circulation Research. 2019;125:855–867. [PubMed: 31600125]
21. Ronaldson-Bouchard K, Ma SP, Yeager K, Chen T, Song L, Sirabella D, Morikawa K, Teles D, Yazawa M and Vunjak-Novakovic G. Advanced maturation of human cardiac tissue grown from pluripotent stem cells. Nature. 2018;556:239–243. [PubMed: 29618819]

22. Bird SD, Doevendans PA, van Rooijen MA, Brutel de la Riviere A, Hassink RJ, Passier R and Mummery CL. The human adult cardiomyocyte phenotype. Cardiovascular Research. 2003;58:423–434. [PubMed: 12757876]

23. Pinto AR, Ilinykh A, Ivey MJ, Kuwabara JT, D'Antoni ML, Debuque R, Chandran A, Wang L, Arora K, Rosenthal NA and Tallquist MD. Revisiting Cardiac Cellular Composition. Circulation Research. 2016;118:400–9. [PubMed: 26635390]

24. Kanisicak O, Khalil H, Ivey MJ, Karch J, Maliken BD, Correll RN, Brody MJ, SC JL, Aronow BJ, Tallquist MD and Molkentin JD. Genetic lineage tracing defines myofibroblast origin and function in the injured heart. Nature Communications. 2016;7:12260.

25. Fu X, Khalil H, Kanisicak O, Boyer JG, Vagnozzi RJ, Maliken BD, Sargent MA, Prasad V, Valiente-Alandi I, Blaxall BC and Molkentin JD. Specialized fibroblast differentiated states underlie scar formation in the infarcted mouse heart. Journal of Clinical Investigations. 2018;128:2127–2143.

26. Kretzschmar K, Post Y, Bannier-Helaouet M, Mattiotti A, Drost J, Basak O, Li VSW, van den Born M, Gunst QD, Versteeg D, Kooijman L, van der Elst S, van Es JH, van Rooij E, van den Hoff MJB and Clevers H. Profiling proliferative cells and their progeny in damaged murine hearts. Proceedings of the National Academy of Sciences of the United States of America. 2018;115:E12245–E12254. [PubMed: 30530645]

27. Glukhov AV, Fedorov VV, Kalish PW, Ravikumar VK, Lou Q, Janks D, Schuessler RB, Moazami N and Efimov IR. Conduction Remodeling in Human End-Stage Nonischemic Left Ventricular Cardiomyopathy. Circulation. 2012;125:1835–1847. [PubMed: 22412072]

28. Lou Q, Fedorov VV, Glukhov AV, Moazami N, Fast VG and Efimov IR. Transmural Heterogeneity and Remodeling of Ventricular Excitation-Contraction Coupling in Human Heart Failure. Circulation. 2011;123:1881–1890. [PubMed: 21502574]

29. Kang C, Qiao Y, Li G, Baechle K, Camelliti P, Rentschler S and Efimov IR. Human Organotypic Cultured Cardiac Slices: New Platform For High Throughput Preclinical Human Trials. Scientific Reports. 2016;6:28798. [PubMed: 27356882]

30. Camelliti P, Al-Saud SA, Smolenski RT, Al-Ayoubi S, Bussek A, Wettwer E, Banner NR, Bowles CT, Yacoub MH and Terracciano CM. Adult human heart slices are a multicellular system suitable for electrophysiological and pharmacological studies. Journal of molecular and cellular cardiology. 2011;51:390–398. [PubMed: 21740909]

31. Ou Q, Jacobson Z, Abouleisa RRE, Tang XL, Hindi SM, Kumar A, Ivey KN, Giridharan G, El-Baz A, Brittian K, Rood B, Lin YH, Watson SA, Perbellini F, McKinsey TA, Hill BG, Jones SP, Terracciano CM, Bolli R and Mohamed TMA. Physiological Biomimetic Culture System for Pig and Human Heart Slices. Circulation Research. 2019;125:628–642. [PubMed: 31310161]

32. Burridge PW, Li YF, Matsa E, Wu H, Ong SG, Sharma A, Holmstrom A, Chang AC, Coronado MJ, Ebert AD, Knowles JW, Telli ML, Witteles RM, Blau HM, Bernstein D, Altman RB and Wu JC. Human induced pluripotent stem cell-derived cardiomyocytes recapitulate the predilection of breast cancer patients to doxorubicin-induced cardiotoxicity. Nat Med. 2016;22:547–56. [PubMed: 27089514]

33. Kitani T, Ong SG, Lam CK, Rhee JW, Zhang JZ, Oikonomopoulos A, Ma N, Tian L, Lee J, Telli ML, Witteles RM, Sharma A, Sayed N and Wu JC. Human-Induced Pluripotent Stem Cell Model of Trastuzumab-Induced Cardiac Dysfunction in Patients With Breast Cancer. Circulation. 2019;139:2451–2465. [PubMed: 30866650]

34. Zhao L and Zhang B. Doxorubicin induces cardiotoxicity through upregulation of death receptors mediated apoptosis in cardiomyocytes. Scientific Reports. 2017;7:44735. [PubMed: 28300219]

35. Barpe DR, Rosa DD and Froehlich PE. Pharmacokinetic evaluation of doxorubicin plasma levels in normal and overweight patients with breast cancer and simulation of dose adjustment by different indexes of body mass. Eur J Pharm Sci. 2010;41:458–63. [PubMed: 20688160]

36. Stemmler HJ, Schmitt M, Willems A, Bernhard H, Harbeck N and Heinemann V. Ratio of trastuzumab levels in serum and cerebrospinal fluid is altered in HER2-positive breast cancer patients with brain metastases and impairment of blood-brain barrier. Anticancer Drugs. 2007;18:23–8. [PubMed: 17159499]

37. Takasaki S, Kawasaki Y, Kikuchi M, Tanaka M, Suzuka M, Noda A, Sato Y, Yamashita S, Mitsuzuka K, Saito H, Ito A, Yamaguchi H, Arai Y and Mano N. Relationships between sunitinib

plasma concentration and clinical outcomes in Japanese patients with metastatic renal cell carcinoma. Int J Clin Oncol. 2018;23:936–943. [PubMed: 29860539]

38. Ou Q, Abouleisa RRE, Tang XL, Juhardeen HR, Meki MH, Miller JM, Giridharan G, El-Baz A, Bolli R and Mohamed TMA. Slicing and Culturing Pig Hearts under Physiological Conditions. J Vis Exp. 2020.
39. Kang C, Qiao Y, Li G, Baechle K, Camelliti P, Rentschler S and Efimov IR. Human Organotypic Cultured Cardiac Slices: New Platform For High Throughput Preclinical Human Trials. Scientific Reports. 2016;6:28798. [PubMed: 27356882]
40. George SA, Brennan JA and Efimov IR. Preclinical Cardiac Electrophysiology Assessment by Dual Voltage and Calcium Optical Mapping of Human Organotypic Cardiac Slices. J Vis Exp. 2020.
41. Morioka MS, Kawaji H, Nishiyori-Sueki H, Murata M, Kojima-Ishiyama M, Carninci P and Itoh M. Cap Analysis of Gene Expression (CAGE): A Quantitative and Genome-Wide Assay of Transcription Start Sites. Methods in molecular biology (Clifton, NJ. 2020;2120:277–301.
42. Li H and Durbin R. Fast and accurate long-read alignment with Burrows-Wheeler transform. Bioinformatics (Oxford, England). 2010;26:589–95.
43. McCarthy DJ, Chen Y and Smyth GK. Differential expression analysis of multifactor RNA-Seq experiments with respect to biological variation. Nucleic Acids Res. 2012;40:4288–97. [PubMed: 22287627]
44. Ritchie ME, Phipson B, Wu D, Hu Y, Law CW, Shi W and Smyth GK. limma powers differential expression analyses for RNA-sequencing and microarray studies. Nucleic Acids Res. 2015;43:e47. [PubMed: 25605792]
45. Unverferth BJ, Magorien RD, Balcerzak SP, Leier CV and Unverferth DV. Early changes in human myocardial nuclei after doxorubicin. Cancer. 1983;52:215–21. [PubMed: 6861067]
46. Chintalgattu V, Rees ML, Culver JC, Goel A, Jiffar T, Zhang J, Dunner K Jr., Pati S, Bankson JA, Pasqualini R, Arap W, Bryan NS, Taegtmeyer H, Langley RR, Yao H, Kupferman ME, Entman ML, Dickinson ME and Khakoo AY. Coronary microvascular pericytes are the cellular target of sunitinib malate-induced cardiotoxicity. Sci Transl Med. 2013;5:187ra69.
47. Li W, Croce K, Steensma DP, McDermott DF, Ben-Yehuda O and Moslehi J. Vascular and Metabolic Implications of Novel Targeted Cancer Therapies: Focus on Kinase Inhibitors. J Am Coll Cardiol. 2015;66:1160–78. [PubMed: 26337996]
48. Uraizee I, Cheng S and Moslehi J. Reversible cardiomyopathy associated with sunitinib and sorafenib. The New England journal of medicine. 2011;365:1649–50. [PubMed: 22030001]
49. Cai F, Luis MAF, Lin X, Wang M, Cai L, Cen C and Biskup E. Anthracycline-induced cardiotoxicity in the chemotherapy treatment of breast cancer: Preventive strategies and treatment. Mol Clin Oncol. 2019;11:15–23. [PubMed: 31289672]
50. Moslehi J and Cheng S. Cardio-oncology: it takes two to translate. Sci Transl Med. 2013;5:187fs20.
51. Geisberg CA and Sawyer DB. Mechanisms of anthracycline cardiotoxicity and strategies to decrease cardiac damage. Curr Hypertens Rep. 2010;12:404–10. [PubMed: 20842465]
52. Groarke J, Tong D, Khambhati J, Cheng S and Moslehi J. Breast cancer therapies and cardiomyopathy. Med Clin North Am. 2012;96:1001–19. [PubMed: 22980061]
53. Pang B, Qiao X, Janssen L, Velds A, Groothuis T, Kerkhoven R, Nieuwland M, Ovaa H, Rottenberg S, van Tellingen O, Janssen J, Huijgens P, Zwart W and Neefjes J. Drug-induced histone eviction from open chromatin contributes to the chemotherapeutic effects of doxorubicin. Nature Communications. 2013;4:1908.
54. Zhang S, Liu X, Bawa-Khalfe T, Lu LS, Lyu YL, Liu LF and Yeh ET. Identification of the molecular basis of doxorubicin-induced cardiotoxicity. Nat Med. 2012;18:1639–42. [PubMed: 23104132]
55. Steinherz LJ, Steinherz PG, Tan CT, Heller G and Murphy ML. Cardiac toxicity 4 to 20 years after completing anthracycline therapy. JAMA. 1991;266:1672–7. [PubMed: 1886191]
56. Cardinale D, Colombo A, Lamantia G, Colombo N, Civelli M, De Giacomi G, Rubino M, Veglia F, Fiorentini C and Cipolla CM. Anthracycline-induced cardiomyopathy: clinical relevance and response to pharmacologic therapy. J Am Coll Cardiol. 2010;55:213–20. [PubMed: 20117401]

57. Horenstein MS, Vander Heide RS and L'Ecuyer TJ. Molecular basis of anthracycline-induced cardiotoxicity and its prevention. Mol Genet Metab. 2000;71:436–44. [PubMed: 11001837]
58. Slamon DJ, Leyland-Jones B, Shak S, Fuchs H, Paton V, Bajamonde A, Fleming T, Eiermann W, Wolter J, Pegram M, Baselga J and Norton L. Use of chemotherapy plus a monoclonal antibody against HER2 for metastatic breast cancer that overexpresses HER2. The New England journal of medicine. 2001;344:783–92. [PubMed: 11248153]
59. Onitilo AA, Engel JM and Stankowski RV. Cardiovascular toxicity associated with adjuvant trastuzumab therapy: prevalence, patient characteristics, and risk factors. Ther Adv Drug Saf. 2014;5:154–66. [PubMed: 25083270]
60. Crone SA, Zhao YY, Fan L, Gu Y, Minamisawa S, Liu Y, Peterson KL, Chen J, Kahn R, Condorelli G, Ross J, Jr., Chien KR and Lee KF. ErbB2 is essential in the prevention of dilated cardiomyopathy. Nat Med. 2002;8:459–65. [PubMed: 11984589]
61. Kurokawa YK, Shang MR, Yin RT and George SC. Modeling trastuzumab-related cardiotoxicity in vitro using human stem cell-derived cardiomyocytes. Toxicol Lett. 2018;285:74–80. [PubMed: 29305325]
62. Pouessel D and Culine S. High frequency of intracerebral hemorrhage in metastatic renal carcinoma patients with brain metastases treated with tyrosine kinase inhibitors targeting the vascular endothelial growth factor receptor. Eur Urol. 2008;53:376–81. [PubMed: 17825982]
63. Moslehi J, Minamishima YA, Shi J, Neuberg D, Charytan DM, Padera RF, Signoretti S, Liao R and Kaelin WG Jr. Loss of hypoxia-inducible factor prolyl hydroxylase activity in cardiomyocytes phenocopies ischemic cardiomyopathy. Circulation. 2010;122:1004–16. [PubMed: 20733101]
64. Barbic M, Moreno A, Harris TD and Kay MW. Detachable glass microelectrodes for recording action potentials in active moving organs. American journal of physiology. 2017;312:H1248–H1259. [PubMed: 28476925]

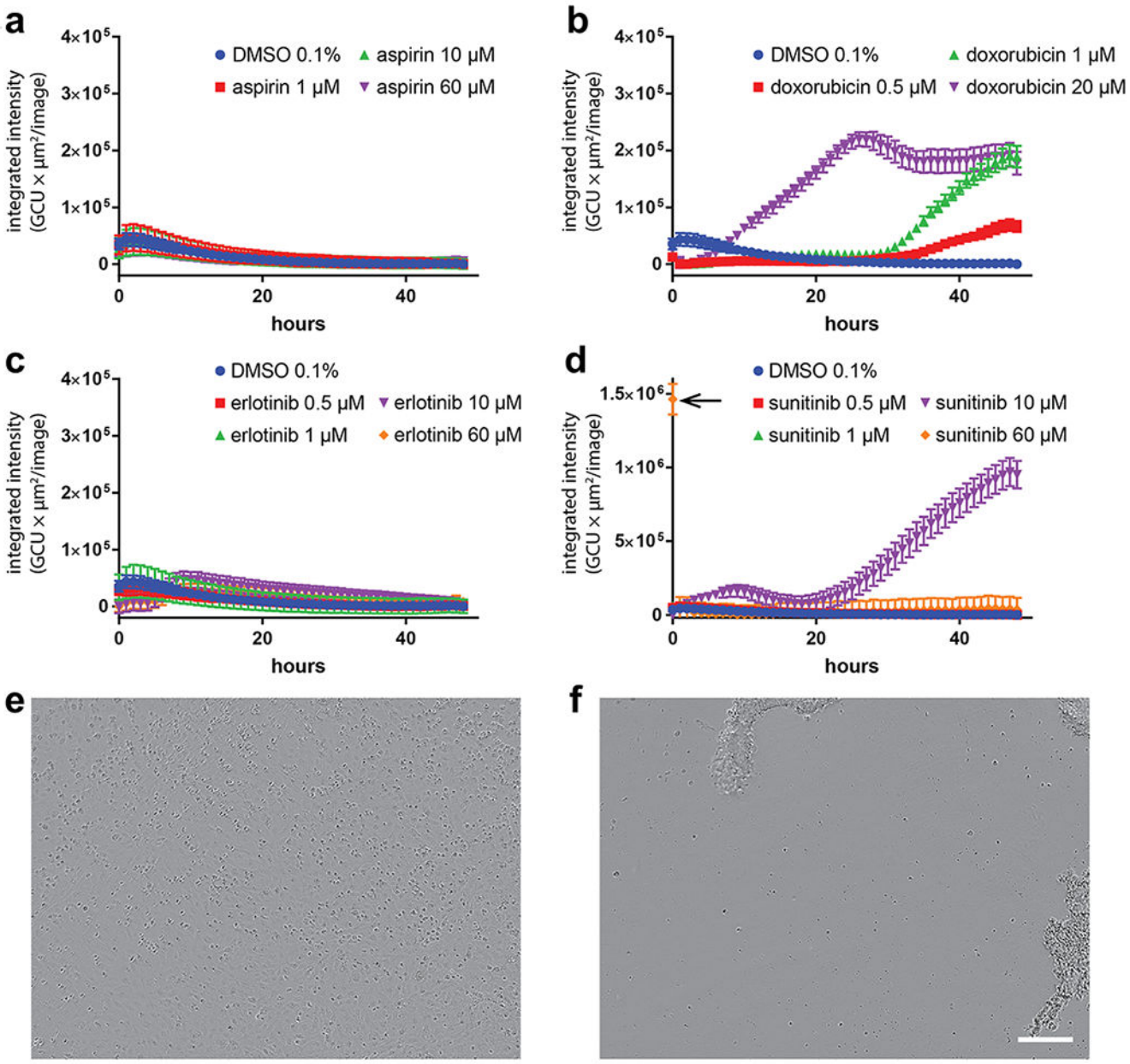

Figure 1. Pro-apoptotic effect of doxorubicin and sunitinib on hiPSC-CMs:

Kinetics of caspase-3/7 activation in hiPSC-CMs exposed to a range of concentrations of **(a)** aspirin (non-toxic drug), **(b)** doxorubicin (cardiotoxin), **(c)** erlotinib (non-cardiotoxic TKI) and **(d)** sunitinib (cardiotoxic TKI) over 48 h. DMSO in the medium at a concentration of 0.1% (v/v) was used as a control. **(a-d)** Variations in total caspase integrated intensity was calculated from fluorescent images of the caspase-3/7 green dye acquired every hour, which captured the extent of apoptosis within cultured cells. Acute apoptotic effects were detected upon exposing cells to 60 μM of sunitinib as noted by the arrow in **(d)**. **(e and f)** Phase microscopy images of cells acquired when 60 μM of sunitinib was added to cells **(e)** and one hour after being exposure **(f)**, where total cell detachment was observed. Scale bar: 200 μm.

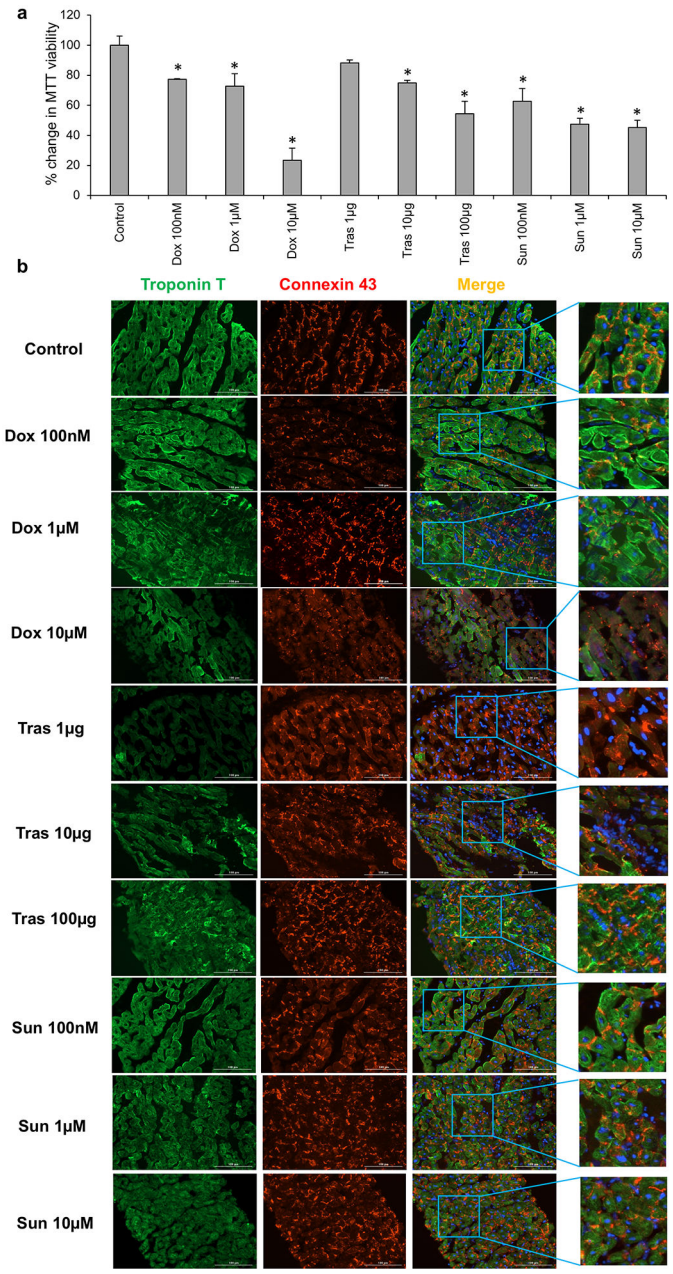

Figure 2. Effect of cardiotoxins on heart slice viability and structure:

(a) Bar graph shows the quantification of heart slice viability after 2 days of treatment with the corresponding cardiotoxin using MTT assay (n=2 independent experiments, 4 replicates in each, One-Way ANOVA test was conducted to compare between groups; *P<0.05 compared to the control). **(b)** Representative immunofluorescence images showing the expression of connexin 43 (red) and Troponin T (green) in cross sections taken from heart tissue slices treated for 2 days with the corresponding concentration of the cardiotoxins (Scale bar, 100 µm). These representative images have been reproducible over 2 independent experiments with 3 technical replicates in each experiment; however, the lack of reliable

tools for quantifying localization of connexin 43 and sarcomeric integrity of troponin T has limited our ability for quantification.

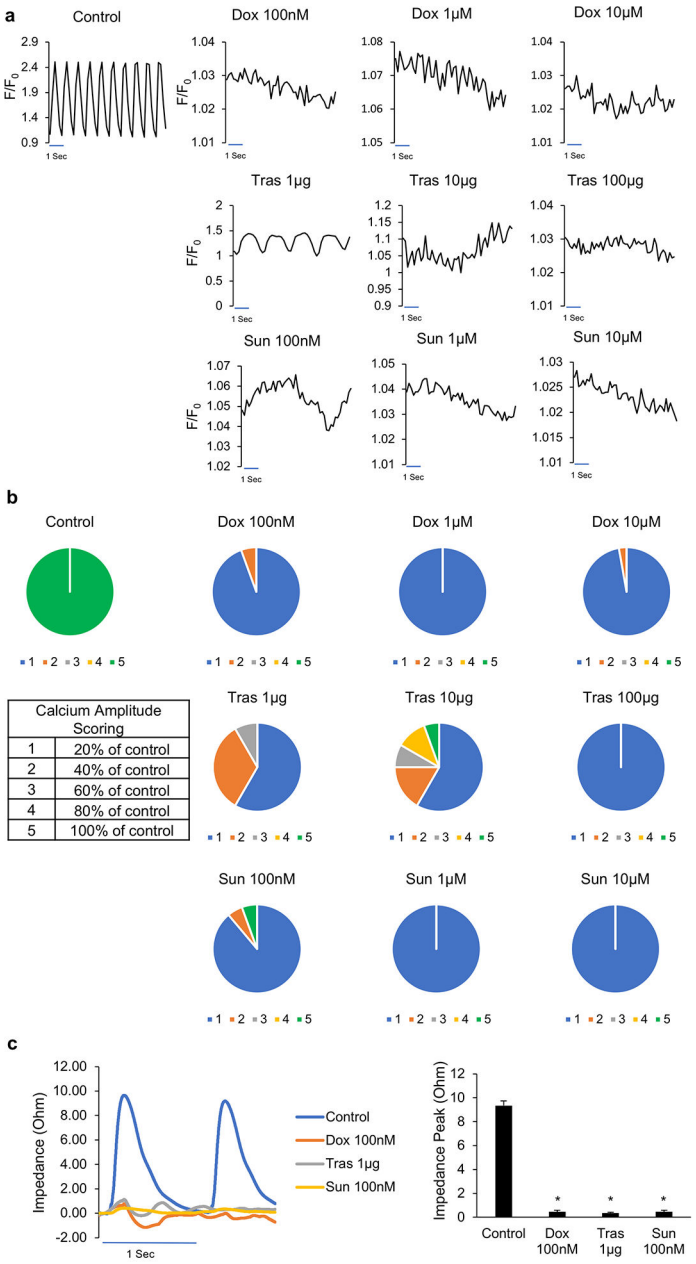

Figure 3. Effect of cardiotoxins on heart slices functionality and calcium homeostasis and contractile function:

(a) Representative calcium traces from day 2 cultured control slices and heart slices treated with the corresponding concentration of each cardiotoxin for 2 days. Transients were recorded after loading the heart slices with Fluo-4 calcium dye and using 1 Hz/20 V electrical stimulation at the time of recording. **(b)** Scoring of calcium transient amplitude as indication of the cardiomyocyte function from slices treated with each cardiotoxin (n=36 cells in each group from 2 independent experiments). **(c)** Left panel, Representative traces of impedance recording for contractile function from slices treated with the low dosages of the three cardiotoxins compared to the control slice. Right panel, shows the quantification of the

contractile force amplitude comparing control slices to the ones treated with the cardiotoxins (n=6 slices, *p<0.05 compared to control).

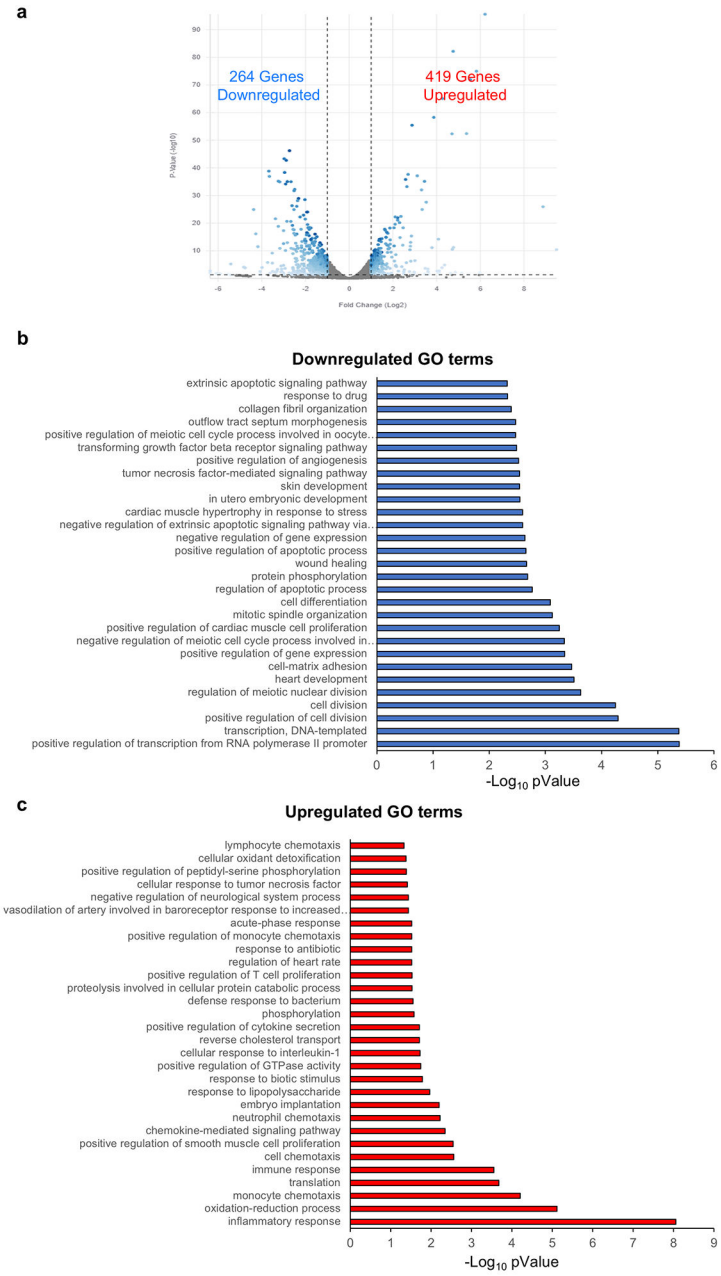

Figure 4. Differential gene expression in slices treated with 100 nM doxorubicin:
(a) Volcano plot showing significant changes in gene expression in 100nM doxorubicin (Dox) treated tissue. Bar graph shows the GO terms for the significantly downregulated **(b)** or upregulated **(C)** genes from RNA-seq data between control heart slices and heart slices treated with 100nM doxorubicin (n=2 pig hearts).

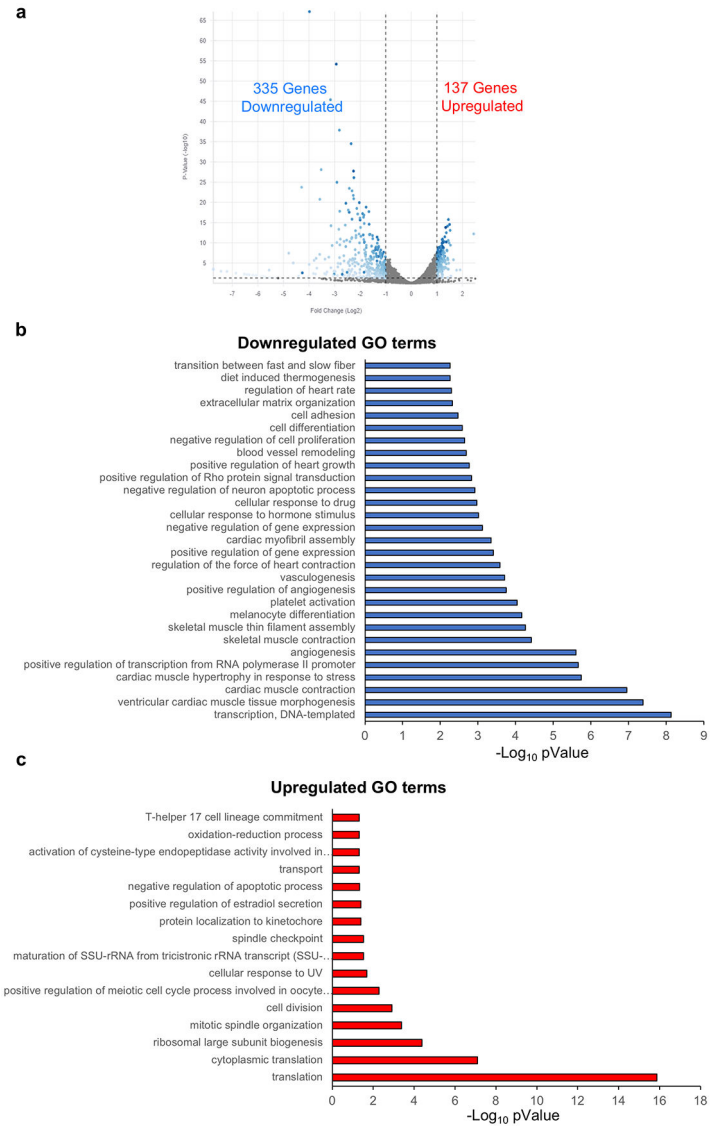

Figure 5. Differential gene expression in slices treated with 1μg trastuzumab:

(a) Volcano plot demonstrating the genes which are significantly different between control heart slice and slices treated with 1μg trastuzumab. Bar graph shows the GO terms for the significantly downregulated **(b)** or upregulated **(c)** genes from RNA-seq data between control heart slices and heart slices treated with 1μg trastuzumab (n=2 pig hearts).

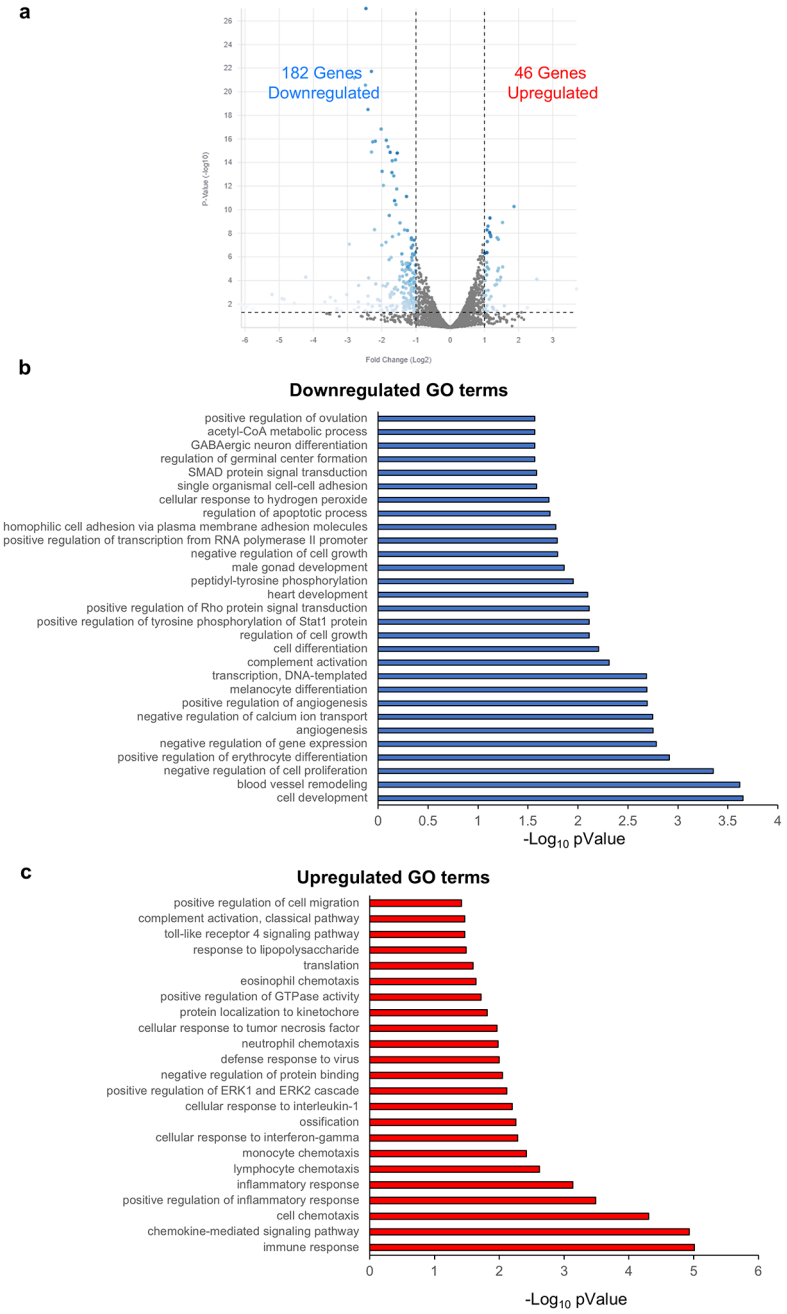

Figure 6. Differential gene expression in slices treated with 100nM sunitinib:

(a) Volcano plot demonstrating the genes which are significantly different between control heart slice and slices treated with 100nM sunitinib. Bar graph shows the GO terms for the significantly downregulated **(b)** or upregulated **(c)** genes from RNA-seq data between control heart slices and heart slices treated with 100nM sunitinib (n=2 pig hearts).

a

Donor No.	1	2	3	4	5	6	7	8	9	10	11
Sex	Male	Male	Male	Male	Male	Male	Male	Male	Female	Female	Female
Age	28	45	50	59	63	64	34	58	62	70	39
Cause of Death	Anoxia	Anoxia	Stroke	Head Trauma	Stroke	Anoxia	Anoxia	Stroke	Stroke	Stroke	Brain Hemorrhage

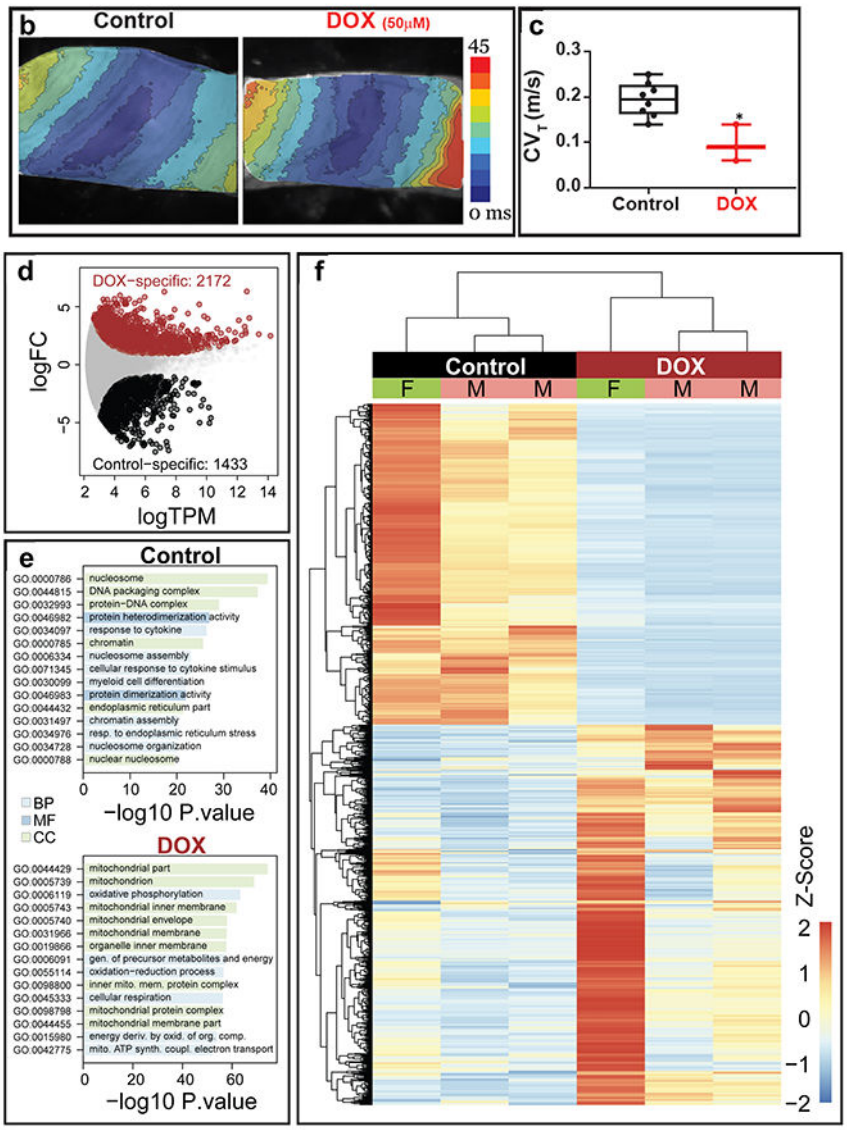

Figure 7. Doxorubicin toxicity in human heart slices:

(a) Age, sex and cause of death for all donated human hearts used in the current study to demonstrate the breadth of variability of the human subjects used in the study. **(b)** Activation maps obtained by optical mapping of human cardiac organotypic slices cultured for ~24 h with or without doxorubicin (50 μM). Crowding of activation lines in the transverse direction indicate conduction slowing with doxorubicin treatment. **(c)** Average transverse conduction velocity determined from human cardiac slices with and without doxorubicin treatment. Transverse conduction velocity was significantly slower in doxorubicin treated slices (n=7, *p<0.05). **(d)** Differentially expressed genes between control and doxorubicin-

treated human cardiac organotypic slices following Cap Analysis of Gene Expression (n=3). **(e)** Gene ontology (GO) enrichment analysis of differentially expressed genes in control and doxorubicin-treated slices. BP: biological process, CC: cellular component, MF: molecular function (n=3). **(f)** Heat map demonstrating hierarchical clustering of differentially expressed genes (n=3). F: female, M: male.